8-9-2006

Building Metal-Anion Layers within a Preovskite Host

Xiao Zhang
University of New Orleans

BUILDING METAL-ANION LAYERS WITHIN A PREOVSKITE HOST

A Thesis

Submitted to the Graduate Faculty of the
University of New Orleans
in partial fulfillment of the
requirements for the degree of

Master of Science
in
The Department of Chemistry

by

Xiao Zhang

B.S. University of Science and Technology of China, 1996

August 2006

Acknowledgement

I would like to express my gratitude to my research advisor Prof. John B. Wiley for his insightful guidance and support during my time at the University of New Orleans. As a true mentor, he helps me on suggesting the topic, providing inspiring ideas, encouraging and supporting my efforts to finish this thesis.

I would like to thank the members of my research committee Profs. Ed Stevens and Matthew Tarr for their helpful advices.

I wish to thank my colleagues Dr. Liliana Viciu, Dr. Feng Li, Dr Doinita Neiner for their fruitful discussions on layered materials chemistry.

I thank all my friends and family members.

Table of Contents

List of Tables

List of Figures

Abstract

Alkali metal halide layers were constructed within Dion-Jacobson (DJ) layered perovskites by a two-step sequential intercalation method. Reductive intercalation with an alkali metal, followed by oxidative intercalation with chlorine gas, leads to the formation of compounds of the general formula, $(A_2Cl)LaNb_2O_7$ (A = Rb, Cs). Rietveld refinement of X-ray powder diffraction data shows that an alkali metal halide layer is formed between the perovskite blocks. The alkali metal cation is eight-coordinate with 4 oxygens from the perovskite layer and 4 chlorides from the new halide layer; this environment is similar to cesium in the CsCl structure. Thermal analysis indicates that these are low-temperature phases where decomposition begins below 200°C. Details on the synthesis and characterization of this set of compounds are presented and the general utility of this approach discussed.

Chapter 1 Introduction and Background

1.1 Perovskites and layered perovskites

Perovskites are mixed oxides with the formula ABO_3 , where A typically corresponds to lanthanides, actinides, alkaline or alkaline earth metals, and B generally corresponds to transition metals.[1] The ideal structure of perovskite-type oxide compound has a Pm3m space group. Its prototype is $CaTiO_3$. Perovskites form one of the most important structure classes in inorganic solid-state chemistry.

The perovskite structure is shown in Figure 1.1. It can be described as a three dimensional network of corner sharing BO_6 octahedra with the A cation twelve-coordinate in the body center. Alternatively, the structure can also be described as a cubic close packed array of anions with the oxygen at the body center replaced by A cation, which is similar in size to oxygen.[2] The close-packed layers are parallel to the (111) planes. One-fourth of the interstitial octahedral sites are filled with the B cations.

The stability of a perovskite oxide depends on the relative sizes of the A and B cations. A tolerance factor *t*, has been empirically defined that allows one to predict the occurrence of the structure for a particular set of cations:

$$t = (R_A + R_O) / \sqrt{2}(R_B + R_O)$$

where R_A, R_B, and R_o are the Shannon and Prewitt ionic radii of the A and B cations and oxygen, respectively. Perovskites are found for values of *t* ranging from 0.8 to 1.1. The flexibility of the perovskite structure is further manifested in its ability to tolerate a relatively large number of defects. Non-stoichiometric phases, in which there is a deficiency or excess of species on the anion or cation sublattice are quite common. Local oxygen displacements, another kind of structural defect, normally accompany cation vacancies and are also present in cation-disordered doped systems when the dopant and host atoms have different radii.

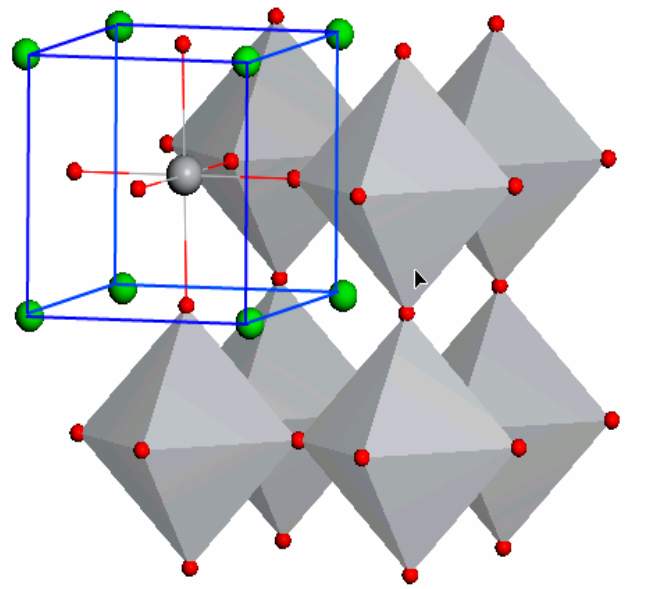

Grey sphere, B sites.
Green sphere, A site,
Red, oxygen.
BO_6 octahedral

Fig 1.1 The perovskite structure ABO_3, unit cell is illustrated. The Octahedral (B sites) and dodecahedral (A Site) coordination is also represented.

The crystal structure and the large number of possible combinations of atom, including mixed-valence pairs, provide for diverse electronic properties. Perovskite-related oxides have been found to exhibit very interesting transport and magnetic properties as well. Colossal magnetoresistance (CMR)[3] is observed in many mixed-valence manganese perovskites, and ferroelectric behavior[4], high-temperature superconductivity[5] and catalytic activity[6] are also shown in perovskite related oxides.

Layered perovskites are intergrowths of perovskite and other structures, and they consist of two-dimensional perovskite slabs interleaved with cations or cationic structure units. The Dion-Jacobson series of layered perovskites[7,8], $A'[A_{n-1}B_nO_{3n+1}]$ (A' = alkali or alkali earth metal, A = rare earth, B = transition metal), has one interlayer cation per formula unit. Ruddlesden-Popper phase[9,10], $A'_2[A_{n-1}B_nO_{3n+1}]$, have two interlayer cations per formula unit and possess twice the interlayer charge density. The number of perovskite layers is given by "n". Fig 1.2 illustrates the structure of Dion-jacobson and Ruddlesden-Popper phase.

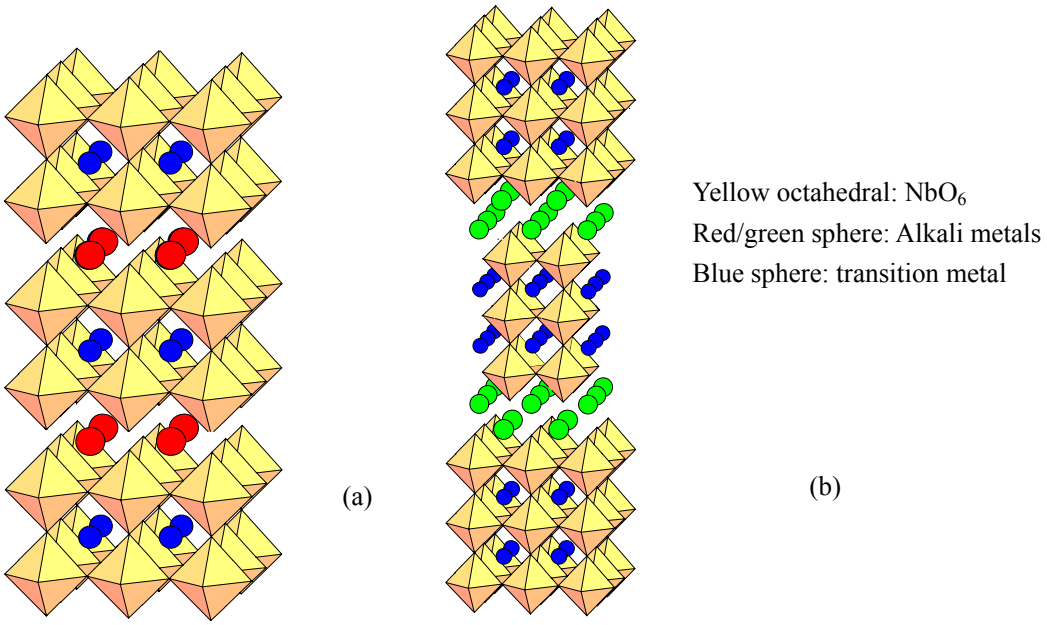

Fig 1.2 Illustration of (a): Double layered Dion-Jacobson phase and (b): Ruddlesden-Popper phase

Double-layered Dion-Jacobson phases A'$LaNb_2O_7$ (A' = alkali metal cations) have been extensively studied. The distinctive feature of these compounds is the electronic configuration of the d^0 transition metal on the B site. It is known that d^0 cation in a octahedral environment has an out-of-center distortion as result of second order Jahn-Teller effect and consequently some of the exciting features of the material containing d^0 cation can be directly traced to this distortion.[11] The phases containing larger interlayer cations such as Cs^+ or Rb^+, favor the formation of layered perovskites because Cs^+ fits better in the large interlayer A-site of a layered perovskite than in the smaller A-site of a three dimensional perovskite. Small cations, such as Li^+ or Na^+ are often difficult to synthesize as phase-pure materials at traditional reaction temperatures (>1000 °C) where three-dimensional perovskites are usually more stable. Smaller cations compounds can only been synthesized by ion exchange reactions. The relative orientation of adjacent perovskite slabs of $ALaNb_2O_7$ can be influenced by the size of the interlayer cation; NbO_6 octahedral in adjacent $LaNb_2O_7^+$ layers are aligned for the larger rubidium and cesium ions phases, partially

staggered for intermediate-sized potassium phase, completely staggered for the smaller lithium and sodium phases[12]. The structure details is shown in Fig. 1.3

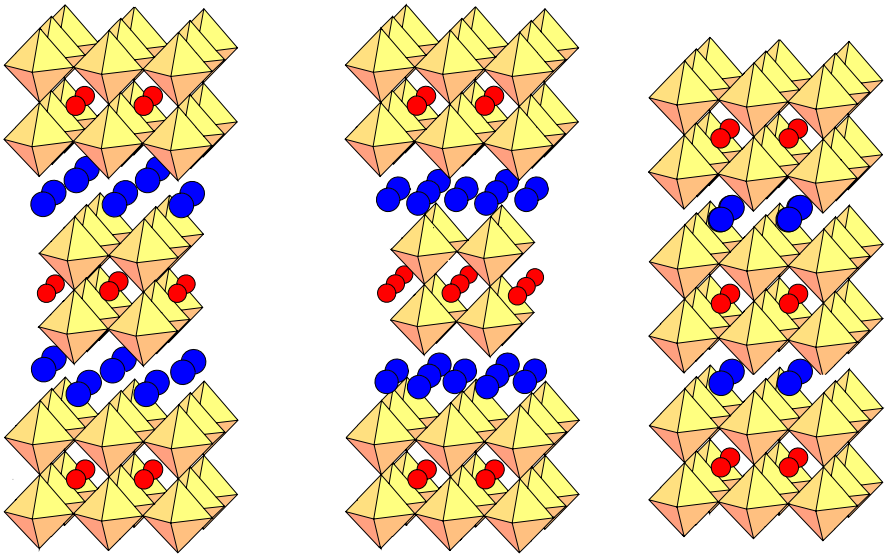

(a) (b) (c)

Fig. 1.3 NbO_6 octahedral alignment in adjacent perovskite blocks. (a):$LiLaNb_2O_7$ (b)$KLaNb_2O_7$ (c):$RbLaNb_2O_7$.Yellow octahedral: NbO_6, Red sphere: Alkali metals, Blue sphere: transition metal

In the alkali metal DJ double layered series the difference between each member arises from the particular mode coordinating the alkali metal within the layer. Therefore, the Cs and Rb members are eight fold coordinated to the apical oxygens of the $Nb(Ta)O_6$ octahedra with full occupancy. In contrast, 50% of the crystallographic A sites are occupied by the alkali ion in the $ALaNb_2O_7$ (A=K, Na, Li) analogues. Potassium ion has a trigonal prismatic coordination whereas the sodium and lithium ions have almost perfect tetrahedral coordination. The tetrahedral coordination in oxides is unique for Na but not for Li. However the tetrahedral coordination of Na ions observed in $NaLaNb_2O_7$ would be essentially unstable at ambient temperature.

1.2 Solid state synthetic method

Availability of pure, well-characterized solid samples is crucial to all solid state studies. Knowledge of the various experimental methods available for the preparation of solids therefore becomes an important and integral part of solid state chemistry. A brief reflection on the development of solid state science reveals that, in many cases, it is the synthesis of a novel compound that has triggered a new line of research.

It is well known that solid state synthesis is quite different than those methods applied in organic or coordinated systems. The most common method used is “heat and beat” high temperature ceramic method. Fine mixing is required in this case, because ceramic reactions are diffusion limited. Thorough grinding is always applied to help increase the contact surface area between reactants. Much of the time in such reactions, intermediate grinding is carried out. Despite its wide spread use, the simple ceramic method has several disadvantages. High temperatures and long reaction time are generally required. This requires a large input of energy. In addition, the phase or compound desired may be unstable or decompose at such high temperatures.

To avoid such a brute force method and obtain better control of structure, stoichiometry and phasic purity, various chemical processes have been developed. Among them are the precursor method, sol-gel method, ion exchange, intercalation/deintercalation, and topochemical methods. These low temperature, chemistry-based approaches, sometimes are called “soft chemistry” (chimie douce). Soft chemistry offers a potentially powerful alternative for controlling those thermodynamically inaccessible structural and morphological features at the kinetic level[13,14].

Topotactic reactions

Solid state reactions differ from those in homogeneous fluid media in a fundamental respect; while reactions in the liquid or the gaseous state depend mainly on the intrinsic reactivity and

concentration of the chemical species involved, solid state reactions depend to a large extent on the arrangement of the chemical constituents in crystals. Chemical reactivity is determined more often by the crystal structure and defect structure of the solid rather than by the intrinsic chemical reactivity of the constituent.

This feature of solid state reactions is clearly brought out in topochemical reactions. "when the reactivity of a solid is controlled by the crystal structure, rather than by the chemical constituents of the crystal, the reaction is said to be *topochemically controlled*" [15]. Thus one can determine the relative positions of the atoms before and after the reaction. And hence deduce the metrical relationships that needed to be satisfied for the reaction to proceed.

Ion exchange

Ion exchange reactions are well known in inorganic solids. It was first reported in 1850. Ion exchange had been restricted to clays and zeolites for many years until it was extended to the inorganic oxides. Some systems exhibiting ion exchange reactions are: lamellar metal oxyhalide FeOCl[16], lamellar niobate $HNb_3O_8 \bullet H_2O$[17], spinel-type material $Li_nMn_{2-x}O_4$[18] and wurtzite-type $NaAlO_2$.[19] In ion exchange reactions, one weakly bonded species can be substituted by another species. These reactions typically are carried out in aqueous or molten salt media. A concentrated exchange liquid aids in overcoming the significant kinetic barrier, the rate determining step is diffusion within the solids. Another important factor of ion-exchange, the thermodynamic aspect, favors exchange between ions of comparable size. In the Dion-Jacobson series, the interlayer cations can easily be exchanged at low temperatures. Actually, Dion-Jacobson phase with small alkali metal Li, Na can only be formed via ion exchange route.[20] Though the kinetic factors usually result in a higher mobility for lower charged cations, identical charges are not necessary. Aliovalent exchange have been reported in our group.[21]

Intercalation

Intercalation is defined as insertion of guest species into the interlayer region of a layered host

while the structure of the layers are essentially maintained. It was first reported in graphite, and then extended in many other systems including layered perovskites. Intercalation refers to a solid state reaction involving reversible insertion of guest species G into a host structure [Hs]. The host provides an interconnected system of accessible unoccupied sites, □. The reaction can be schematically represented as

$$x\ G + \square_x\ [Hs] \rightarrow G_x[Hs]$$

The reaction is considered to be topotactic because the host matrix retains its integrity with respect to structure and composition in the course of intercalation and disintercalation. Since the 1960's, intercalation chemistry has received wide attention, in view of it significance in a number of technically important problems such as reversible electrodes for high-energy density batteries, superconductivity and catalysis. A wide variety of inorganic solids such as layered transition-metal oxides, chalcogenides, halides, oxyhalides, layered silicates, zeolites and even metal alloys have been used as host materials[15]. Guest species range from simple atomic species such as hydrogen, alkali metals and halogens, through neutral molecules to complex organometallics.

Reductive intercalation with alkali metals

Alkali metals are very popular intercalation candidates due to their unique chemical and physical properties. Since they are very strong reductive reagents, the intercalation processes are always accompanied by reduction of transition metals, which can result in mixed valence products. Herein we briefly introduced the process for alkali metal reductive intercalation. Appropriate amount of alkali metal was weighed out on a piece of Pyrex tubing (6mm of) for ease of handling, combined with DJ phase $ALaNb_2O_7$, the combination was placed in a Pyrex tube (12mm od) along with 0.2g of sample, and the tube was sealed under vacuum. The excess alkali metal partly compensated the loss due to reaction with the glass. There was no physical contact between the powder and alkali metal. Fig.1.4 illustrates the arrangement. The Pyrex tube was then heated for enough time in different temperatures. The Pyrex tube was periodically rotated to expose fresh sample surfaces to the alkali metal vapor. The mixed

valence product had a homogeneous dark gray color. Unreacted metal was distilled away from the product by heating the sample tube in a temperature gradient. The intercalation reagents and products were all handled in an argon-filled dry box to minimize the air and moisture exposure.

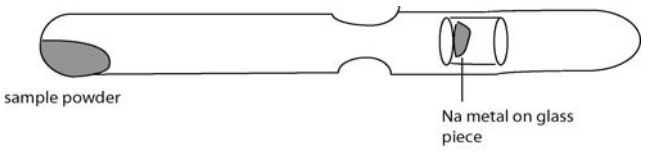

Fig. 1.4 Reductive intercalation occurs in Pyrex turbe

Chlorine and oxygen oxidative intercalation

Both oxygen and chlorine gas are active oxidative reagents, that can be used to produce mixed valenced compounds. The reductive intercalation products were oxidized with chlorine gas, the procedure is briefly described here. The reaction set up[22] is illustrated in Fig. 1.5. Reactants were measured and sealed into a bottle with rubber cap in argon filled dry box. The bottle was then connected into reaction flask by two cannulas. First, nitrogen was flowed for about 30 minutes to remove all the air in reaction system. After that, chlorine gas is introduced into the system. The reaction temperature is controlled by an oil bath and the unreacted chlorine was treated by NaOH solution. Reaction is often indicated by a color change, the black sample cha became white on full oxidation. After the reaction had been finished, the system was flushed with nitrogen to remove the remaining chlorine gas.

Oxidation with oxygen can be carried out in a Pyrex tube analogously to what is shown in Figure 1.4, with a carefully calculated amount of Ag_2O or $KClO_3$ treated in different temperatures.

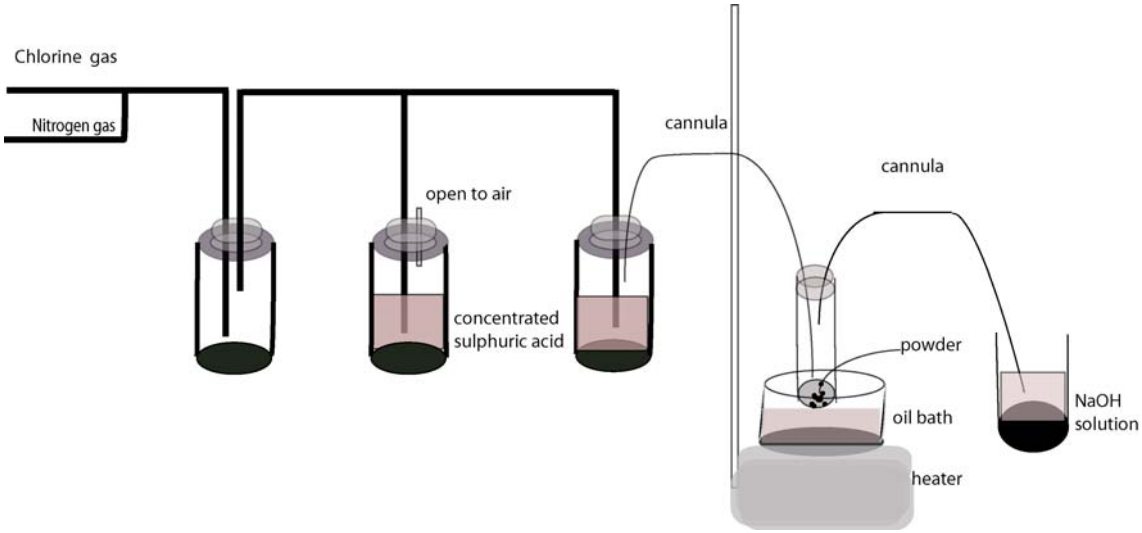

Fig.1.5. Chlorine oxidation apparatus set up. Three bottles are used to control the gas flow rate and avoid overpressure. Cannula is used to introduce gas to reaction system while keep airtight. Temperature can be controlled by oil bath or heating element.

1.3 Crystallography

Once a material is obtained, its characterization is the essential part of all investigation in the solid state chemistry. The most important step in characterization of a material is structural determination. Various methods can be used to represent the crystal structure. Among those the unit cell approach gives the most common interpretion. In this approach, crystal structures represent a regular three-dimensional arrangement of atoms. This arrangement can be seen as repeating units, and they are called the unit cell, which can be defined as "the smallest repeating unit which shows the full symmetry of the crystal structure".

Symmetry

There are seven unique crystal systems, which reflect the symmetry of crystals while not including the positions of the atoms in the unit cell. There are cubic, hexagonal, tetragonal, trigonal, orthorhombic, monoclinic and triclinic.

Table 1.1 The seven crystal systems[2]

Crystal system	Unit cell shape	Essential symmetry	Space lattice
Cubic	$a=b=c$, $\alpha=\beta=\gamma=90^o$	Four threefold axes	P, F, I
Tetragonal	$a=b\neq c$, $\alpha=\beta=\gamma=90^o$	One fourfold axis	P, I
Orthorhomic	$a\neq b\neq c$, $\alpha=\beta=\gamma=90^o$	Three twofold axes or mirror planes	P, F, I, A (B or C)
Hexagonal	$a=b\neq c$, $\alpha=\beta=90^o$, $\gamma=120^o$	One sixfold axis	P
Trigonal (a)	$a=b\neq c$, $\alpha=\beta=90^o$, $\gamma=120^o$	One threefold axis	P
(b)	$a=b=c$, $\alpha=\beta=\gamma\neq 90^o$	One threefold aoxs	R
Monoclinic	$a\neq b\neq c$, $\alpha=\beta=90^o$, $c\neq 90^o$	One two fold axis or mirror plane	P, C
Triclinic	$a\neq b\neq c$, $\alpha=\beta=\gamma\neq 90^o$	None	P

The symbols in this column stand for P-primitive, F-all face centered, I-body centered, R-rombohedral, A-A face centered, B-B face centered, C-C face centered.

Bravais lattice

An array of points can represent the repetition of atoms, ions or molecules in the crystals and they are called lattice points. The lattice points together with the crystal systems give the *Bravais lattice* (periodic array of the repeated units such as single atoms, groups of atoms, molecules, ions, etc.), which appears exactly the same from whichever of the points is viewed of a structure. There are fourteen possible Bravais lattices (e.g. primitive monoclinic or face centered cubic, etc.).

Based on the symmetry elements which operates in a crystal system, there are 230 possible space groups accounting for the site atoms in a particular crystalline lattice.

Miller indices

Consider the three-dimensional array of lattice points. The array of points may be divided up into many different sets of planes, and for each set there is a characteristic perpendicular distance, d, between pairs of adjacent planes, which is called interplanar d-spacing. Lattice planes are labeled by Miller indices to each set. The derivation of Miller indices is illustrated in fig 1.6

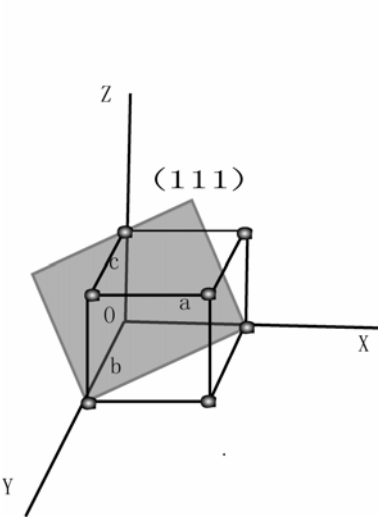

Fig 1.6. examples of derivation of miller indices (111)

Consider that plane which is adjacent to the one that passes through the origin. Find the intersection of this plane on the three axes of the cell and write these intersections as fractions of the cell edges. In this case, the plane cuts the x axis at a, y axis at b and the z axis at c. the fractional intersection are 1/1, 1/1,1/1, take reciprocals of these fractions ,this gives (111). These three integers are the miller indices of the plane.

Directions in lattices are labeled by first drawing a line passes through the origin which parallel to the direction. The line pass through a point with general fractional coordinates x, y, z, [x y z] are the indices of the direction. [hkl] direction is always perpendicular to the (hkl) plane in cubic system.

For different crystal system, d spacing is calculated from Table 1.2

Table 1.2 Interpalanr spacing

Unit cell	Interplanar spacing
Cubic	$1/d^2 = \frac{h^2+k^2+l^2}{a^2}$
Tetragonal	$1/d^2 = \frac{h^2+k^2}{a^2} + \frac{l^2}{c^2}$
Orthorhombic	$1/d^2 = \frac{h^2}{a^2} + \frac{k^2}{b^2} + \frac{l^2}{c^2}$
Hexagonal	$1/d^2 = \frac{4}{3}\frac{h^2+hk+k^2}{a^2} + \frac{l^2}{c^2}$
Monoclinic	$1/d^2 = \frac{1}{\sin^2\beta}[\frac{h^2}{a^2} + \frac{k^2\sin^2\beta}{b^2} + \frac{l^2}{c^2} - \frac{2hl\cos\beta}{ac}]$
Triclinic	$1/d^2 = \frac{1}{V^2}[h^2b^2c^2\sin^2\alpha + k^2a^2c^2\sin 2\beta + l^2a^2b^2\sin 2\gamma + 2hkabc^2(\cos\alpha\cos\beta - \cos\gamma) + 2kla^2bc(\cos\beta\cos\gamma - \cos\alpha) + 2hlab^2c(\cos\alpha\cos\gamma - \cos\beta)]$

.

1.4 Characterization method

X-ray Diffraction

X-ray diffraction represents the most powerful techniques used in phase recognition. X-rays are electromagnetic radiation of wavelength ~ 1Å. Monochromatic X-rays are used in almost all diffraction experiments. A beam of accelerated electrons is driven to strike a metal target, often copper. It has sufficient energy to ionize the copper 1s electrons, then an outer orbital electron drops to occupy the vacant 1s orbital while emitting X-radiation. These transition energies have fixed values equal to copper 2p→1s or transition 3p→1s transition, called K_α and K_β, respectively. The K_α radiation occurs more frequently and is a doublet due to slightly different energy for two spin states of 2p electron which makes the transition. The intensity-weighted

average is 1.5418Å.

When wavelike radiation hits on a sample having a regular lattice, diffraction effects may occur. While X-rays are scattered mainly by electrons that surround atomic nuclei, neutrons are scattered either by the atomic nucleus or by a magnetic field in the sample. The scattering power for the X-rays is proportional to the electron density of the sample under investigation and therefore heavier atoms with more electrons scatter more strongly than the lighter elements.

When X-rays come across an atom, they are scattered in all directions and the result is a set of scattered beams, which are in phase with one another. A radiation beam coming to a sample having a regular array of scattering centers gives rise to constructive interference of the radiation if the radiation has a similar wavelength with the sample periodicity. The condition for constructive interference of the radiation is usually expressed in terms of Bragg's law:

$$n\lambda = 2d\sin\theta,$$

where λ is the monochromatic radiation, d is the regularly spaced planes of the scattering centers, n is an integer called the order of reflection and θ is the angle of incident beam of the atomic planes involved.

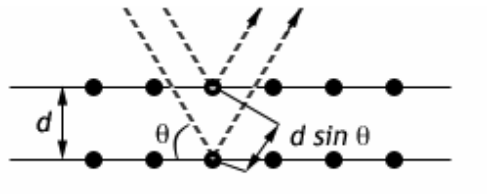

Fig 1.7 the diffraction geometry. The parallel atomic planes are separated by d, and the beam has the incidence angle θ. The path difference between the optical beams for two plane is $d\sin\theta$.

A powder pattern has two characteristic features, the d spacings which are characteristics of the unit cell, and their intensities, which are characteristic for the arrangement of atoms in a specific unit cell. The intensity of the scattered radiation depends upon the nature of the interaction with the sample and the internal structure of the material.

Intensity

Each electron in an atom scatters X-rays and the scattering intensity is a sum of the individual intensities. The scattering factor also called form factor, *f*, for an atom is proportional with the number of the constituent electrons. The path difference for the two beams was found to be 2dsinθ, and for constructive interference to occur this difference must be an integer multiple of the wavelength.

However, there may be further scattering centers present in the sample, which do not satisfy this criterion. To quantify their effects, the phase of the scattered wave from any arbitrary point is determined and then a summation over all points in the sample is carried out. Measuring the phase difference for the two scattered waves in radians gives $\delta = 2\pi(2\mathbf{r}\sin\theta)/\lambda$, where **r** is the vector connecting the points. For a given direction of the scattering, a vector **r*** may be defined with $\mathbf{r}^* = 2\sin e/\lambda$ and $\delta = 2\pi r^* r$. The wave may be written mathematically as $A\exp(i\varphi)$, where A is the amplitude and $\boldsymbol{\varphi}$ is the phase, the summation over all scatterers in the sample becomes:

$$F(\mathbf{r}^*) = \sum f_i \exp(i\delta) = \sum f_i \exp(i2\pi\mathbf{r}^*\mathbf{r}) = \int \rho(r)\exp(i2\pi\mathbf{r}^*\mathbf{r})d\mathbf{r}$$

f_i gives the scattering power of the particular point. The sum may be written as an integral when the scattering density is continuous (e.g. electron density, ρ(r)). The relationship between the diffracted waves and the sample scattering density is a Fourier transform. The expression may now be used to find the intensity of a diffracted beam in any arbitrary sample byusing the relationship $I \propto |F|^2$.

The structure factor equation relates the intensity of the diffracted beam to the internal structure of the material. This comes from the first part of the equation for F(**r***), after **r*** is replaced by *hkl* the structure factor F(**r***) is changed to F(*hkl)*.

$$F(hkl) = \sum f_i \exp(2\pi i(hx + ky + lz))$$

Where f_i is form factor and the sum is carried out over all the unit cell.

Rietveld refinement

Rietveld refinement is a widely used method for polycrystalline samples refinement. In this method, the powder diffraction profile for the structural model is calculated by taking into account the following factors: a) lattice parameters - to determine peak positions; b) atomic position and thermal parameters - to determine peak intensities; c) 2θ dependent analytical functions – to describe the peak shapes and peak widths; d) a description of the background intensity. The pseudo-Voight function is most extensively used function for the peak shape of the X-ray powder diffraction data because it allows the variation of both Gaussian and Lorentzian character. To describe the 2θ dependence of the peak width, analytical functions are also used. The excitement of Rietveld method is that the calculated powder diffraction pattern is compared point by point, with the experimental powder diffraction, and selected parameters defining the structural model and describing the profile are adjusted by least-square methods to give the best fit. The agreement between the experimental and calculated powder diffraction patterns is commonly expressed by some factors. The R factor (R_p), the weighted R factor (R_{wp}), and χ^2 are defined as the following:

profile, $R_p = \sum [y_{io} - y_{ic}] / \sum y_{io}$;

weighted profile, $R_{wp} = [\sum w_i (y_{io} - y_{ic})^2 / \sum w_i (y_{io})^2]^{1/2}$

goodness of fit (GOF), $\chi^2 = [R_{wp} / R_{\exp}]^2$. $R_{\exp} = [(N-P) / \sum w_i y_{io}^2]^{1/2}$,

y_{io} and y_{ic} are the observed and calculated intensities, w_i is the weighting factor, N is the total number of y_{io} data when the background is refined, and P is the number of adjusted parameters.

EDS (Energy Dispersive Spectrometry)

Energy Dispersive Spectroscopy (EDS) is a standard procedure for identifying and quantifying elemental composition of sample areas as small as a few cubic micrometers. Characteristic X-rays are produced for each element when a material is bombarded with electrons in an

electron beam instrument, such as those produced with a scanning electron microscope (SEM). Detection of these X-rays can be accomplished by an energy dispersive spectrometer, which is a solid state device that discriminates among X-ray energies.

1.5 Purpose of this research

DJ double layered compounds of general formula $ALaM_2O_7$[12,23] (where A= H, alkali metal, NH_4, Ag, Pyridine, n-amine, $C_nH_{2n+1}^+$ and M = Nb^{5+}, Ta^{5+}) as well as triple layered compounds, $ACa_2M_3O_{10}$[7,8] (where A = H, alkali metal, n-amines and M = Nb^{5+}, Ta^{5+}) are known. In the alkali metal DJ double layered series the difference between each member arises from the particular fashion in which the alkali metal is coordinated within the interlayer. The Cs and Rb members are eight fold coordinated to the apical oxygens of the $Nb(Ta)O_6$ octahedra with all A sites occupied, while 50% of the crystallographic A sites are occupied by the alkali ion in the $ALaNb_2O_7$ (A = K, Na, Li) analogues. Potassium ion has a trigonal prismatic coordination whereas the sodium and lithium ions adopt almost perfect tetrahedral coordination.

The distinctive feature of these compounds is the electronic configuration of the d^0 transition metal on the B site. It is known that d^0 cation in a octahedral environment has an out of center distortion as result of second order Jahn-Teller effect[24] and consequently some of the exciting features of the material containing d^0 cation can be directly traced to this distortion. Gopalakrishnan and coworkers[12] showed that the formation of layered structures exhibiting ion-exchange and intercalation as well as Brønsted acidity is a direct consequence of the MO_6 octahedra deformation which results in unequal M-O bonds (two different M-O bond length on the z axis and four ordinary M-O bond length in the xy plane). Since the oxygens of the shorter M-O bonds on z axis are less basic relative to other oxygens, protons attached to these sites can readily intercalate amines between layers. By intercalating long chain amine between layers, the DJ compounds have been expanded and individual crystallites can exfoliate to form very thin sheets in the direction perpendicular to the layers.[25] All of these layered perovskite compounds

are suitable systems for investigation of two-dimensional physical properties, such as ion conduction[26] and luminescence[27]. Since these physical properties can be controlled by ion-exchange, the compounds are thought to be good candidates for new heterogeneous catalysis and ionic conductors.

The new interest in DJ compounds started in 1999 when it was demonstrated that they can coexchange both cations and anions to form $(MX)LaNb_2O_7$[28] (M = Cu; X =Cl, Br). The new structure contains CuO_2X_4 octahedra that corner-share with NbO_6 octahedra from the perovskite layer and edge-share with each other along all four equatorial edges.

Multistep reaction strategies involving a combination of ion exchange and reductive intercalation have also been utilized to construct lithium and sodium chloride layers within DJ hosts. Herein we report a new approach to the fabrication of metal halide arrays within receptive hosts. Multistep reactions based on sequential intercalation steps can be used to construct new metal-anion layers; reductive intercalation followed by oxidative intercalation of layered perovskite hosts produces new layered perovskites containing alkali halide layers with a cesium-chloride-like structural features. We have also examined the oxidative intercalation of oxygen, and extended the strategy to other DJ compounds.

1.6 References

[1] Galasso, F. S., *Properties and preparation of Pervoskite-type compounds.* Pergamon Press: Oxford: **1969**;

[2] West, A. R., *Solid State Chemistry and its Application*. John Wiley & Sons Ltd: **1987**;

[3] Maignan, A.; Martin, C.; Damay, F.; Raveau, B., *Chem. Mater.* **1998,** 10, 950;

[4] Moritomo, Y.; Asamitsu, A.; Kuwahara, H.; Tokura, Y., *Nature* **1996,** 380, 141.

[5] Bednorz, J. G.; Muller, K. A. Z., *Phys. B* **1986,** 64, 189;

[6] Horn, J.; Zhang, S. C.; Selvaraj, U.; messing, G. L.; Trolier-Mckinstry, S., *J. Am. Chem. Soc.* **1999,** 82, 921.

[7] Dion, M.; Ganne, M.; Tournoux, M. *Mater.Res.Bull*., **1981**, *16*, 1429;

[8] Dion, M.; Ganne, M. ; Tournoux, M.; Revez, J. *Rev. Chim. Miner.* **1984**, *21*, 92.

[9] Ruddlesden, S.N. and Popper, P. *Acta Crystallogr*., **1957**, *10*, 538.

[10] Gopalakrishnan , J. ; Bhat, V.; *Inorganic Chem.* **1987**, *26*, 4301.

[11] Bhuvanesh, N. S. P., Gopalakrishnan, J. *J. Mater. Chem*., **1997**, *7(12)*, 2297.

[12] Gopalakrishnan, J. and Bhat, V. *Mat. Res. Bull.*,**1987**, *22*, 413.

[13] Stein, A. Keller, S.W.; Mallouk, T.E. *Science* **1993**, *259*, 1558.

[14] Gopalakrishnan, J. *Chem. Mater.* **1995**, *84*, 141.

[15] Rao. C.N.R. and Gopalakrishnan, J. *New Directions in Solid State Chemistry* 2nd ed. Cambrige University Press:

1997

[16] Kanamura, K.; Sakaebe, H.; Zhen, C.; Takehara, Z., *Journal of the Electrochemical Society* **1991,** *138*, 2971.

[17] Nedjar, R.; Borel, M. M.; Raveau, B., *Mater. Res. Bull.* **1985,** *20*, 1291.

[18] Feng, Q.; Miyai, Y.; Kanoh, H.; Ooi, K., *Langmuir* **1992,** *8*, 1861.

[19] Villafuerte-Castrejon, M. E.; Aragon-Pina, A., *Materials Research Society Symposium Proceedings* **1992,** , (271).

[20] Gopalakrishnan, J.; Bhat, V.; Raveau, B., *Mater. Res. Bull.* **1987,** *22*, 413.

[21] McIntyre, R. A.; Falster, A. U.; Li, S.; Simmons, W. B.; O'connor, C. J.; Wiley, J. B., *J. Am. Chem. Soc.* **1998,** *120*, 217.

[22] Jolly, W.L. *The Synthesis and Characterization of Inorganic Compounds;* Prentice-Hall, Inc., **1970**.

[23] Cushing, B. L.; Wiley, J. B.; *Mater. Res. Bull*, **1999**, *34*, 271.

[24] Kang, S. K.; Tang, H.; Albright, T. A.; *J. Am. Chem. Soc*., **1993**, *115*, 1971

[25] Treacy, M. M. J.; Rice, S. B.; Jacobson, A. J.; Lewandowski, J. T.; *Chem. Mater*., **1990**, *2*, 279.

[26] a)Toda, K.; Kurita, S.; Sato, M.; *Solid State Ionics*, **1995**, *81*, 267; b)Toda, K.; Watanabe, J.; Sato, M.; *Solid State Ionics*, **1996**, *90*, 15; c)Toda, K.; Suzuki, T.; Sato, M.; *Solid State Ionics*, **1997**, *93*, 177.

[27] a)Toda, K.; Kameo, Y.; Ohta, M.; Sato,M.; *J. Alloys Compound*, **1995**, *218*, 228; b) Kudo, A.; *Chem. Mater*,

1997, *9*, 664.

[28] a) Kodenkandath, T. A.; Lalena, J. N.; Zhou, W. L.; Carpenter, E. E.; Sangregorio, C.; Falster, A. U.; Simmons, W. B.; O'Connor, C. J.; Wiley, J. B.; *J. Am.Chem. Soc*, **1999,** *121*, 10743; b) Kodenkandath, T. A.; Kumbhar, A. S.; Zhou, W. L.; Wiley, J. B.; *Inorg. Chem*., **2001**, *40*, 710; c) Kodenkandath, T. A.; Viciu, M. L.; Zhang, X.; Sims, J. A.; Gilbert, E. W.; Augrain, F. X.; Chotard, J. N.; Caruntu, G.; Sinu, L.; Zhou, W. L.; Wiley, J. B.; *Mat. Res. Soc. Symp. Proc.,* **2001**, *658*, GG8.5.1; d) Viciu, M. L.; Caruntu, G.; Koenig, J.; Zhou, W. L.; Kodenkandath, T. A.; Wiley, J. B., *Inorg. Chem* **2002,** *41*, 3385. e) Viciu, M. L.; Koenig, J.; Spinu, L.; Zhou, W. L.; *Chem. Mater.* **2003,** *15*, 1480.

Chapter 2

Building Metal-Anion Layers within a Perovskite Host by Sequential Intercalation

2.1 Introduction

Topochemical reactions, such as ion exchange and intercalation, are powerful tools for performing structural modifications on receptive host compounds. Recently researchers have been quite effective in the manipulation of a variety of perovskite systems with these methods[1, 2]. Reactions with layered perovskites of the Ruddlesden-Popper $A_2[A'_{n-1}B_nO_{3n+1}]$ (RP) [3, 4], Dion-Jacobson $A[A'_{n-1}B_nO_{3n+1}]$ (DJ) [5, 6], and Aurivillius $Bi_2O_2[A'_{n-1}B_nO_{3n+1}]$[7, 8]structure types have been especially fruitful. These sets of compounds readily undergo ion exchange and the DJ series are also receptive to reductive intercalation. One goal among current researchers has been to use such layered hosts as templates for directing the growth of new metal-anion arrays; the formation of such layers can be viewed analogously to epitaxial thin film growth, though here the new layer forms within a crystal versus on the crystal surface. Some of the initial reports in this area have involved the formation of transition metal halide and metal oxide layers. Metal halide layers (MX; M = V, Cr, Mn, Fe, Co, Cu; X = Cl (Br)) have been constructed within DJ hosts by ion exchange with simple metal halides (MX_2) to produce compounds such as $(MX)LaNb_2O_7$.([9-13]) Metal-oxide layers have been inserted into layered perovskites by reactions with mixed metal oxyhalides [14 15]; $Ca_2La_2CuTi_2O_{10}$, for example, has been prepared from $NaLaTiO_4$ and $Ca_2CuO_2Cl_2$ [15]. Multistep reaction strategies involving a combination of ion exchange and reductive intercalation have also been utilized to construct lithium and sodium chloride layers within DJ hosts [16 17]. Herein we report a new approach to the fabrication of metal halide arrays within receptive hosts. Multistep reactions based on sequential intercalation steps can be used to construct new metal-anion layers; reductive intercalation followed by oxidative intercalation of layered perovskite hosts produces new layered perovskites containing alkali halide layers with a cesium-chloride-like structural features.

2.2 Experimental

2.2.1 Sample Preparation.

The Dion-Jacobson phase, $RbLaNb_2O_7$, was prepared by a method similar to that reported in the literature. [18] Initially, La_2O_3 and Nb_2O_5 were heated at 1050°C for 12 h to remove absorbed water and carbonates, then stoichiometric quantities of La_2O_3 (Alfa, 99.99%) and Nb_2O_5 (Alfa, 99.9985%), with a 25% molar excess of Rb_2CO_3 (Alfa, 99%), were thoroughly ground together, annealed at 850°C for 12 h, and heated at 1050°C for 24 h. The excess of Rb_2CO_3 was added to balance that lost due to volatilization. After the reaction, the solid product was washed thoroughly with distilled water and dried at 150°C overnight. The cesium analogue was prepared by the same procedure as rubidium, starting from Cs_2CO_3 (Alfa, 99.994%). The other members of the series, $ALaNb_2O_7$ (A = Li, Na, K), were obtained by ion exchange from $RbLaNb_2O_7$ and the corresponding alkali metal nitrates in a 10:1 molar ratio. $LiLaNb_2O_7$, $NaLaNb_2O_7$ and $KLaNb_2O_7$ were prepared with $LiNO_3$ (Alfa, 99.98%), $NaNO_3$ (Alfa, 99.0%) and KNO_3 (Alfa, 99.0%), at 300°C, 400°C and 350°C for 2 days, respectively. [12 18] The resulting products were washed with distilled water and dried at 100°C overnight. The completion of the ion-exchange reaction was confirmed by X-ray powder diffraction; the unit cells of the products were in good agreement with published values[18].

2.2.2 Reductive Intercalation.

The series $A_2LaNb_2O_7$ (A = Li, Na, K, Rb, Cs) was prepared by reductive intercalation. $Rb_2LaNb_2O_7$ was obtained by intercalation of $RbLaNb_2O_7$ with Rb metal vapor. [19] Varying amounts (10, 2, 1.5, 1-fold molar ratio) of alkali metal were weighed out onto pieces of Pyrex tubing (6 mm o.d., open both ends) for ease of handling, the combination was placed in a Pyrex tube (12mm o.d.) along with 0.2 g of $RbLaNb_2O_7$ sample, and the tube was sealed under vacuum ($< 10^{-4}$ torr). The excess alkali metal partly compensated the loss due to reaction with the glass. There was no physical contact between the powder and alkali metal. The Pyrex tube was then heated for 3 days at 200ºC. The tube was periodically rotated to expose fresh sample

surfaces to the alkali metal vapor. The product $Rb_2LaNb_2O_7$ had a homogeneous blue-black color. Unreacted metal was distilled away from the product by heating the sample tube in a temperature gradient for 7 days. The Na, K and Cs analogues were prepared by a similar procedure, except that due to slight differences in melting points for the alkali metals, samples were heated for 4 days at 300ºC, 250ºC and 200ºC, respectively. The intercalation reagents and products were all handled in an argon-filled dry box to minimize exposure to water and oxygen; the intercalation products are especially air sensitive. Lithiation to form $Li_2LaNb_2O_7$ from $LiLaNb_2O_7$ was performed using an excess of n-BuLi (Aldrich 1.6 M in hexanes) in a solution of hexane [20]. The reaction was maintained under constant stirring at ambient temperature on a Schlenk line under argon atmosphere for 1 day and subsequently washed many times with hexanes before drying.

2.2.3 Oxidative Intercalation.

The reductive intercalation products, $A_2LaNb_2O_7$, were reacted with chlorine gas (Matheson, 99.99%). In the case of $Rb_2LaNb_2O_7$, about 0.2 g of compound was loaded under argon into a 40 ml scintillation vial fitted with a TFE/silicone septa cap. The vial was connected to a gas system by two stainless steel cannulas and purged with nitrogen for about 30 minutes before the introduction of chlorine gas. The chlorine gas was bubbled through sulfuric acid in a system similar to that described by Jolly [21] . The $Rb_2LaNb_2O_7$ sample was initially blue-black in color but changed to white after a 1 h chlorine treatment at room temperature. The system was then flushed with nitrogen to purge the remaining chlorine gas. The unreacted chlorine was scrubbed out with a 10 M NaOH solution. (*Warning: chlorine is a highly toxic, corrosive gas that should be handled with extreme caution.* [22]) The cesium analog was prepared in a similar fashion. $Li_2LaNb_2O_7$, $Na_2LaNb_2O_7$ and $K_2LaNb_2O_7$, however, did not oxidize even at elevated temperatures up to 100 ºC.

2.2.4 Characterization.

X-ray powder diffraction data were collected on a Philips X'Pert System equipped with a graphite monochromator and Cu Kα radiation (λ = 1.5418Å). Typical scans were collected in continuous mode from 5 to 95°2θ with a scan rate of 0.02°/s. Peak positions were determined with the program PROFILE FIT [23] and lattice parameters were refined by a least-squares method. The crystal structures were refined by the Rietveld method with GSAS.[9] The refined parameters were scale factor, zero-point shift, 8 background parameters, peak shape parameters, cell parameters, and atomic coordinates. Regions between 26.930-27.910 and 38.730- 39.110° 2θ were excluded due to the presence of small amounts of impurities.

The products were found to be insoluble in a variety of acids even though they were maintained in acidic solutions for several days. Therefore, the elemental analysis was carried out by energy dispersive spectroscopy (EDS) of several individual crystallites. EDS analysis was performed on a JEOL JSM 5410 scanning electron microscope equipped with an EDAX-DX Prime microanalytical system.

Differential scanning calorimetry (DSC) was carried out in flowing argon on a Netzsch 404S thermal analysis system. Samples were heated at a rate of 10°C/min in alumina pans.

2.3 Results

2.3.1 Synthesis.

$Rb_2LaNb_2O_7$ is known to readily form by reductive intercalation of $RbLaNb_2O_7$ with excess Rb metal vapor (Eq. 2.1). [19]

$$RbLaNb_2O_7 + Rb^0 \rightarrow Rb_2LaNb_2O_7 \qquad \text{(Eq. 2.1)}$$

$Rb_2LaNb_2O_7$ is then be oxidatively intercalated with chlorine gas to produce $(Rb_2Cl)LaNb_2O_7$ (Eq. 2.2).

$$Rb_2LaNb_2O_7 + 1/2Cl_2 \rightarrow (Rb_2Cl)LaNb_2O_7 \qquad \text{(Eq. 2.2)}$$

X-ray diffraction data showed that the product was always accompanied by a small amount of RbCl byproduct. It was thought that this byproduct might come from the use of an excess of Rb metal in the reductive intercalation step where some residual metal remains on the sample surface even though the sample was heated in a temperature gradient. A series of $Rb_2LaNb_2O_7$ samples, prepared from various amounts of Rb metal, was then reacted with chlorine. It was found that the sample prepared with close to 1:1.2 ratio of Rb metal greatly reduced the RbCl impurity, though a very small amount could still be observed in the powder diffraction patterns (Figure 2.1). Elemental analysis by EDS indicated that the relative composition of the compound was 1.92:0.95:1.0:2 for Rb:Cl:La:Nb.

The two-step intercalation process can also be applied to $CsLaNb_2O_7$ to produce $(Cs_2Cl)LaNb_2O_7$, though the resulting product is less crystalline. For $LiLaNb_2O_7$, $NaLaNb_2O_7$ and $KLaNb_2O_7$, the corresponding $A_2LaNb_2O_7$ are all known, but none of them showed evidence of oxidation with chlorine even with long reaction times and elevated temperatures.

2.3.2 Structural Characterization.

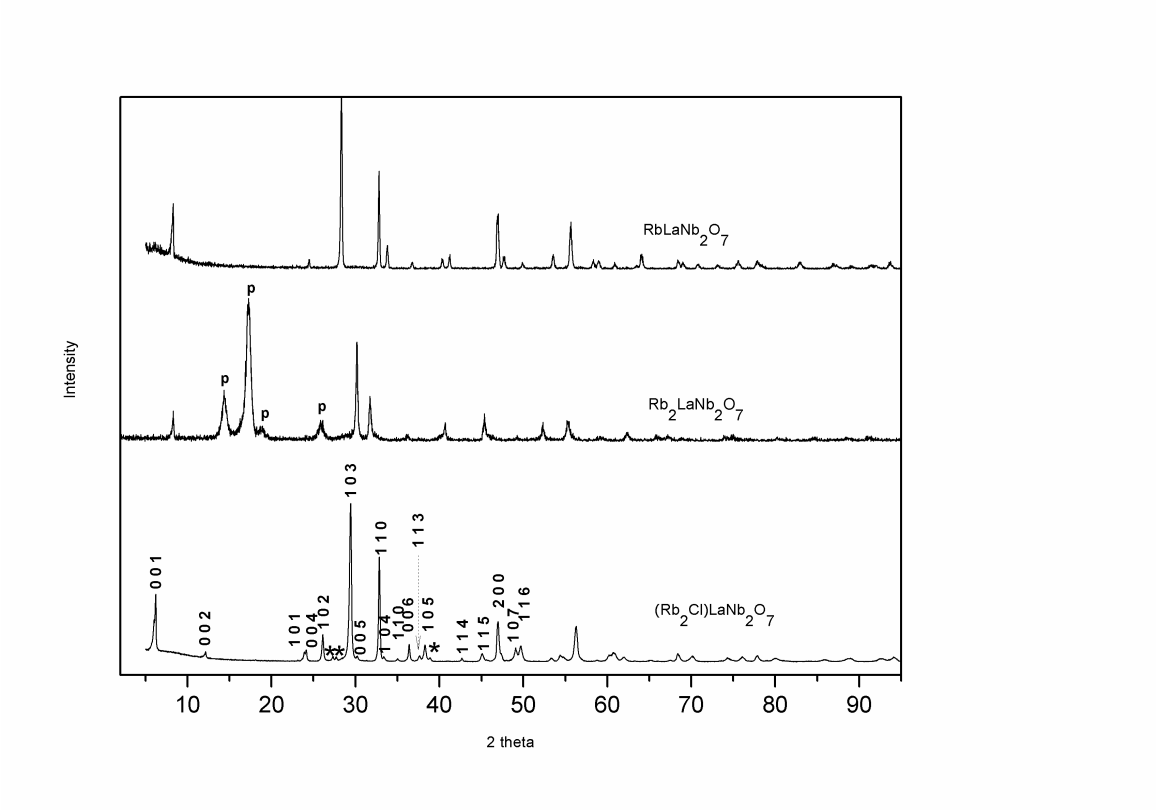

Figure 2.1. X-ray powder diffraction data for (a) $RbLaNb_2O_7$, and the intercalation products (b) $Rb_2LaNb_2O_7$ and (c) $(Rb_2Cl)LaNb_2O_7$. $Rb_2LaNb_2O_7$ is a calculated pattern from reference [19]. Miller indices are indicated for select reflections of $(Rb_2Cl)LaNb_2O_7$; asterisks (*) indicate minor RbCl impurity, peaks marked as "p" come from polymer which covered the surface of $Rb_2LaNb_2O_7$ during measurement

Figure 2.1 shows a comparison of the powder diffraction patterns for $RbLaNb_2O_7$, $Rb_2LaNb_2O_7$ and $(Rb_2Cl)LaNb_2O_7$. The reflections in $(Rb_2Cl)LaNb_2O_7$ could readily be indexed on a tetragonal unit cell (Table 2.1). A large expansion in the *c* parameter (*ca.* 3.94 Å) occurred relative to the starting material $RbLaNb_2O_7$. Though several possible structural models were considered based on the bonding preferences of rubidium and the degree of layer expansion, the model where rubidium was contained in cubic coordination was found to give the best match. Rietveld refinement was then carried out on this model in the P4/mmm space group; refined data

are presented in Figure 2,2 and Table 2.2.

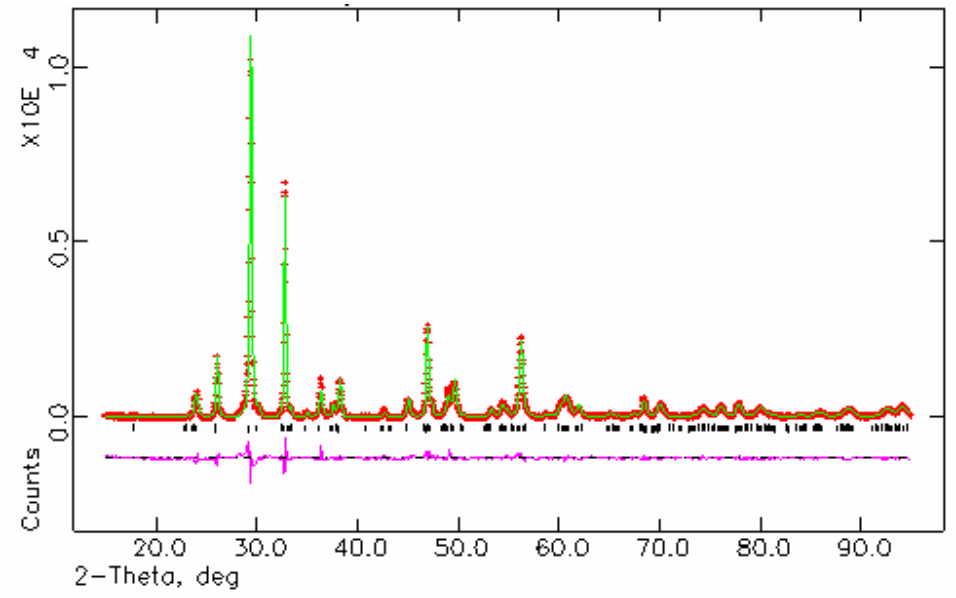

Fig. 2.2 Rietveld refinement plot for $(Rb_2Cl)LaNb_2O_7$. Crosses indicate observed data and a solid line indicates the calculated pattern; the difference plot is shown at the bottom.

Table 2.1. Tetragonal Unit Cell Parameters for the parent and the Exchange Product

compound	unit cell (Å)		cell volume
	a	*c*	(Å^3)
$RbLaNb_2O_7$[a]	3.896	11.027	167.4
$Rb_2LaNb_2O_7$[b]	4.029	11.555	187.6
$(Rb_2Cl)LaNb_2O_7$	3.889(1)	14.917(2)	225.7(1)

[a]values from reference [18] [b]converted from orthorhombic cell in reference [19].

Table 2.2. Crystallographic data for $(Rb_2Cl)LaNb_2O_7$[a]

atom	site	x	y	Z	g	$U_{iso}(Å^2)$
Rb	2g	0	0	0.3648(2)	1	0.0261(10)
La	1a	0	0	0	1	0.0098(8)
Nb	2h	1/2	1/2	0.1517(1)	1	0.0054(10)
O1	4i	0	1/2	0.1252(7)	1	0.013(3)
O2	2h	1/2	1/2	0.270(1)	1	0.018(5)
O3	1c	1/2	1/2	0	1	0.075(10)
Cl	1d	1/2	1/2	1/2	1	0.024(3)

[a]P4/mmm; Z = 1 R_p = 9.51%; R_{wp} = 12.95%; χ^2 = 4.456;
g is occupation factor.

Figure 2.3 shows the $(Rb_2Cl)LaNb_2O_7$ structure. The perovskite blocks are maintained during the two-step intercalation process while a new double layer of rubidium chloride (Rb_2Cl) was constructed within the interlayer. Here the rubidium resides in an eight coordinate site, similar to cesium in the CsCl structure, except that the rubidium is bound to 4 chlorides from the new halide layer and 4 oxygens from the perovskite block. The chloride also has cubic coordination being surrounded by eight rubidium cations. Metal-anion bond distances are provided in Table 2.3. The Rb–O distance (3.092(2) Å) is shorter than the average distance reported for the $RbLaNb_2O_7$ parent compound (3.129 Å), while the Rb–Cl (3.410(7) Å) distances are long relative to those of the simple binary compound RbCl (3.291 Å), respectively. The coordination in the latter compound, however, is octahedral rather than cubic. The cesium compound (a = 3.894(4) Å, c = 15.19(2) Å) appears isostructural to $(Rb_2Cl)LaNb_2O_7$.

Table 2.3. Selected Bond Distances for $(Rb_2Cl)LaNb_2O_7$

bond type	bond distance (Å)
Rb - Cl	3.410(2)
Rb – O2	3.092(7)
La – O1	2.696(7)
La – O3	2.750(1)
Nb - O1	1.984 (2)
Nb - O2	1.77(1)
Nb - O3	2.262(2)

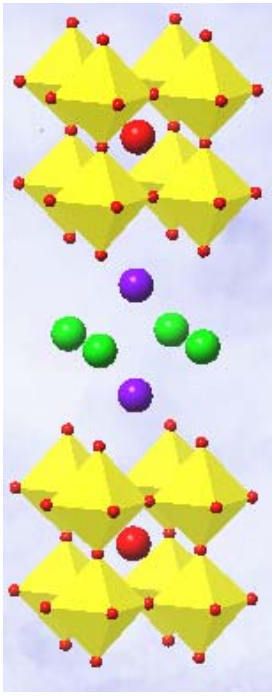

Figure 2.3. Structure of $(Rb_2Cl)LaNb_2O_7$ where large red spheres are lanthanum cations, small red spheres are oxygens, green spheres are chlorines and purple are rubidiums. The octahedra represent NbO_6.

2.3.3 Thermal analysis.

$(Rb_2Cl)LaNb_2O_7$ is a low temperature phase. After annealing at various temperatures under argon, XRD shows that this compound starts to decompose by 200 °C. On decomposition, RbCl and the poorly crystalline parent compound, $RbLaNb_2O_7$, are produced. At higher temperatures, DSC shows a reversible endotherm at 716 °C corresponding to the melting point of RbCl.

2.4 Discussion

A new approach is presented for the construction of metal-anion arrays within receptive perovskite hosts. A two-step sequential intercalation method involving both reductive and oxidative intercalation is used. While the reductive step has been reported by other researchers, [19] the oxidative step, especially when used in this tandem approach, is significant in that it leads to for the formation of metal-anion layers. Here we have demonstrated this with

the construction of rubidium chloride and cesium chloride layers within a double-layered perovskite.

This sequential intercalation method appears to be dependent on the precursor used. Oxidative intercalation reactions with other $A_2LaNb_2O_7$ (Li, Na, K) did not occur up to 100 °C. This is likely related to the smaller layer spacing associated with this set of compounds relative to those of the rubidium and cesium; the layer spacings are 10.16, 10.45, 10.77, 11.105, and ? for Li, Na, K, Rb, Cs, respectively. Previously, our group has shown that both $(Li_xCl)LaNb_2O_7$ and $(Na_xCl)LaNb_2O_7$ can be prepared by reductive intercalation of $(CuCl)LaNb_2O_7$ [17]. The initial introduction into the perovskite layer of the relatively large chloride ion, by ion exchange of $RbLaNb_2O_7$ with $CuCl_2$ [9] prior to the reductive intercalation step appears to be important in accessing the lithium and sodium halide compounds. Efforts to prepare $(Rb_xCl)LaNb_2O_7$ from $(CuCl)LaNb_2O_7$ were not successful, and resulted in a mixture of several phase. This result also indicates that with the larger alkali cations, it is better to introduce the cation into the layer prior to that of the anion.

It is known that the use of low-temperature (< 500 °C) topotactic reactions can lead to the synthesis of low temperature as well as metastable phases. [15] [14] Many of these reactions were carried out above 300 °C and typically lead to compounds that decompose by 700 °C. In the case of $(Rb_2Cl)LaNb_2O_7$, the oxidative intercalation step was carried out at room temperature. Such lower reaction temperatures might prove to be important in that they could expand the synthetic window available for exploring new compounds. This is confirmed here where $(Rb_2Cl)LaNb_2O_7$ is a low temperature phase that shows evidence of decomposition by 200 °C – several hundreds of degrees lower than seen in other systems.

The sequential reductive and oxidative intercalation reactions allow the construction of an A_2Cl layer intermediate to the perovskite blocks. The coordination of rubidium in $(Rb_2Cl)LaNb_2O_7$

with these layers is eight coordinate (i.e., RbO_4Cl_4). While cubic geometry is seen for rubidium in the parent, $RbLaNb_2O_7$, in simple binary chloride, RbCl, the coordination is octahedral. It is only with the larger cesium cation in the CsCl structure that cubic coordination is observed. The square oxygen base of the perovskite block likely directs rubidium into this coordination. One can view this as an "internal epitaxy" where the geometry of the host directs the structure of the new rubidium halide layer.

The reaction strategy presented here exploits a sequential set of reductive and oxidative intercalation reactions for the construction of new metal halide layers within a perovskite host. The extension of this approach to other hosts and different sets of intercalants should lead to new compounds. ([25]: Preliminary results indicate that this method can be extended to triple DJ perovskites series as well as a the intercalation of oxygen.) Further, the idea of repetitive reductive/oxidative processes to continuously add a series of new layers to a host is intriguing. Such methodologies would not only allow the fabrication of structurally interesting materials, but could lead to magnetically and electronically properties in rationally designed compounds.

2.5 References

[1] V. Caignaert, F. Millange, B. Domenges, B. Raveau, and E. Suard, *Chem. Mater.*, **1999**, *11*, 930.

[2] L. Iordanidis and M. G. Kanatzidis, *J. Am. Chem. Soc.*, **2000**, *122*, 8319.

[3] S. N. Ruddlesden and P. Popper, *Acta Crystallogr.*, **1957**, *10*, 538.

[4] S. N. Ruddlesden and P. Popper, *Acta Crystallogr.*, **1958**, *11*, 54.

[5] M. Dion, M. Ganne, and M. Tournoux, *Mater. Res. Bull.*, **1981**, *16*, 1429.

[6] M. Dion, M. Ganne, M. Tournoux, and J. Ravez, *Rev. Chim. Miner*, **1984**, *21*, 92.

[7] B. Aurivillius, *Ark. Kemi*, **1949**, *1*, 499.

[8] B. Aurivillius, *Ark. Kemi*, **1949**, *1*, 463.

[9] T. A. Kodenkandath, J. N. Lalena, W. L. Zhou, E. E. Carpenter, C. Sangregorio, A. U. Falster, W. B. Simmons, C. J. O'connor, and J. B. Wiley, *J. Am. Chem. Soc.*, **1999**, *121*, 10743.

[10] T. A. Kodenkandath, A. S. Kumbhar, W. L. Zhou, and J. B. Wiley, *Inorg. Chem*, **2001**, *40*, 710.

[11] T. A. Kodenkandath, M. L. Viciu, X. Zhang, J. A. Sims, E. W. Gilbert, F.-X. Augrain, J.-N. Chotard, G. A. Caruntu, L. Spinu, W. L. Zhou, and J. B. Wiley, *Proc. Mater. Res. Soc. Symp.*, **2001**, 658.

[12] M. L. Viciu, G. Caruntu, J. Koenig, W. L. Zhou, T. A. Kodenkandath, and J. B. Wiley, *Inorg. Chem*, **2002**, *41*, 3385.

[13] M. L. Viciu, J. Koenig, L. Spinu, W. L. Zhou, and J. B. Wiley, *Chem. Mater.*, **2003**, *15*, 1480.

[14] J. Gopalakrishnan, T. Sivakumar, K. Ramesha, V. Thangadurai, and G. N. Subbanna, *J. Am. Chem. Soc.*, **2000**, *122*, 6237.

[15] T. Sivakumar, S. E. Lofland, K. V. Ramanujachary, K. Ramesha, G. N. Subbanna, and J. gopalakrishnan, *J. Solid State Chem.*, **2004**, *177*, 2635.

[16] M. L. Viciu, V. Golub, T. A. Kodenkandath, and J. B. Wiley, *Mater. Res. Bull.*, **2004**, *39*, 2147.

[17] M. L. Viciu and J. B. Wiley, *unpublished work*, .

[18] J. Gopalakrishnan, V. Bhat, and B. Raveau, *Mater. Res. Bull.*, **1987**, *22*, 413.

[19] A. R. Armstrong and P. A. Anderson, *Inorg. Chem*, **1994**, *33*, 4366.

[20] M. Sato, T. Jin, and H. Ueda, *Chem. Lett.*, **1994**, *4*, 161.

[21] W. L. Jolly, in 'The Synthesis and Characterization of Inorganic Compound', Prentice-Hall, Inc., **1970**.

[22] A. C. Larson and R. B. Von Dreele, in 'General Structure Analysis System (GSAS)', **2000**.

[23] E. J. Sconneveld and R. Delhez, in 'ProFit', **1996**.

[24] A. F. Wells, in 'Structural Inorganic Chemistry. 5th ed.', Oxford University Press, **1984**.

[25] X. Zhang and J. B. Wiley, ACS Meeting, **2005**

Vita

The author was born in Dangshan, Anhui province, China in April 1975. In 1991, he began undergraduate study in material science and engineering at the University of Science and Technology of China, majored in materials chemistry. He received his BS degree in 1996. In the summer of 2000, he came to the University of New Orleans and joined Professor John B. Wiley's research group